Review Article

The role of diffusion weighted magnetic resonance imaging in oncologic settings

Zulkif Bozgeyik, Mehmet Ruhi Onur, Ahmet Kursad Poyraz

Firat University, Elazığ, Turkey

Corresponding to: Zulkif Bozgeyik. University of Firat, Faculty of Medicine, Department of Radiology, 23119, Elazig-Turkey. Email: bozgeyik4@hotmail.com.

Abstract: There is growing interest in the applications of diffusion-weighted-imaging (DWI) in oncologic area for last ten years. DWI has important advantages as do not require contrast medium, very quick technique and it provides qualitative and quantitative information that can be helpful for tumor assessment. In this article, we present oncologic applications of DWI in the parts of the body. DWI has been applied to the evaluation of central nervous system (CNS) pathologies. Some technologic advances lead to using of DWI in the extracranial sites such as abdomen and pelvis. As well as tumor detection and characterization, DWI has been widely used for predicting and monitoring response to therapy. One of the most prominent contributions of DWI is differentiation of between malignant and benign tumoral process. Apparent-diffusion-coefficient (ADC) value is quantitative parameter of DWI which reflects diffusion movements of water molecules in various tissues. Most of the studies suggested that malignant tumors had lower ADC values than benign ones. DWI may be a routine sequence in oncologic settings and it provides much useful information about tumoral tissue. We think it can be added to conventional magnetic resonance imaging (MRI) sequences.

Keywords: Diffusion-weighted MRI; oncology; magnetic resonance imaging (MRI)

Submitted Oct 04, 2013. Accepted for publication Oct 20, 2013.
doi: 10.3978/j.issn.2223-4292.2013.10.07
Scan to your mobile device or view this article at: http://www.amepc.org/qims/article/view/2913/3831

Introduction

Diffusion-weighted-imaging (DWI) provides microscopic information from water protons which is not possible using conventional magnetic resonance imaging (MRI). DWI measures the random (Brownian) extra, intra and transcellular motion of water molecules (1). Apparent-diffusion-coefficient (ADC) is a quantitative parameter calculated from DWI combines the effects of capillary perfusion and water diffusion (2). ADC value is calculated for each pixel of the image and is displayed as a parametric map. By drawing regions of interests on these maps, the ADCs of different tissues can be derived (3).

In biologic tissues, the DWI signal is derived from the motion of water molecules in the extracellular space, intracellular space and intravascular space (2). Tumors have increased vascularity. So, significant proportions of signal on DWI originated from intravascular space (4). The degree of restriction to water diffusion is correlated with tissue cellularity and integrity of cell membranes (5). Generally, malignant tumors have enlarged nuclei and show hypercellularity. These histopathologic characteristics reduce the extracellular matrix and the diffusion space of water protons in the extracellular areas, with a resultant decrease in the ADC value (6,7).

As well as tumor detection and characterization, DWI has been widely used for predicting and monitoring response to therapy. Many researchers have reported that DWI has potential for evaluating tumor response during treatment. Increase of ADC value was accepted as response to therapy in many animal studies (8). Also, results of many clinical studies show that increase in the ADC value suggest a better treatment outcome in clinical studies (9,10).

DWI has been applied to the evaluation of central nervous system (CNS) pathologies especially in stroke, for

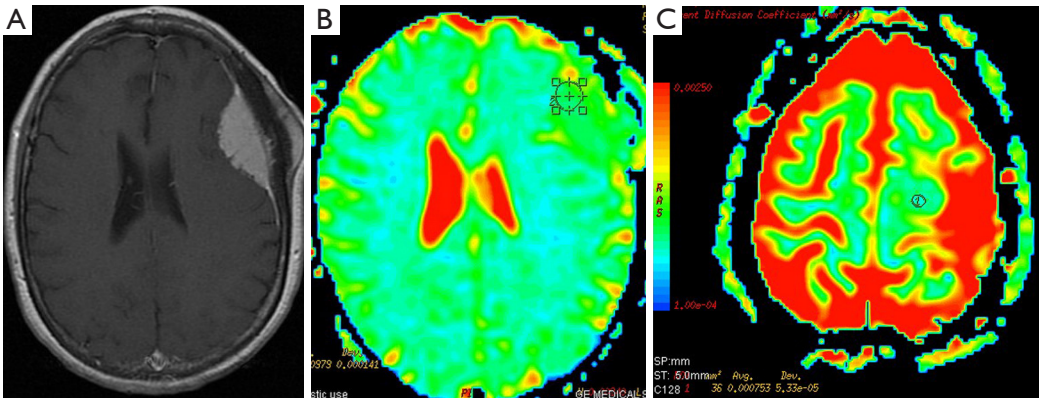

Figure 1 (A,B) Typical meningioma is located at left convexity; (A) Contrast enhanced axial T1 weighted image shows hyperostosis of bone neighbouring of the lesion and hyperintense lesion with hyperintense dural tail; (B) ADC map of the lesion. Mean ADC value of the lesion is 0.97×10^{-3} mm^2/s; (C) Atypical meningioma located on the left parietal area. Color ADC map. ADC value of the lesion is 0.75×10^{-3} mm^2/s. Abbreviation: ADC, apparent-diffusion-coefficient.

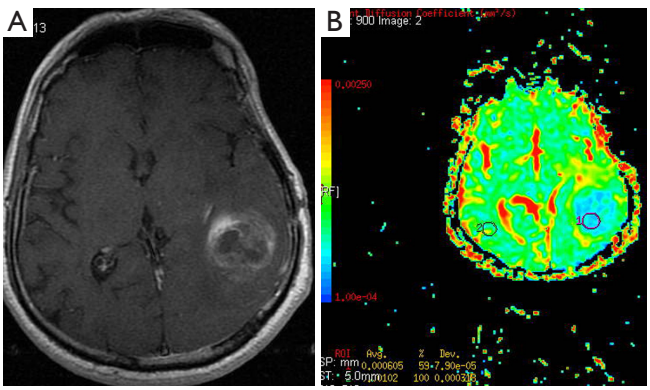

Figure 2 A 61-year old man with glioblastoma multiforme proven histopathologically. (A) Contrast enhanced T1 weighted image shows heterogenous and irregular enhancement of the lesion; (B) The lesion has lower ADC value (0.6×10^{-3} mm^2/s) than ADC value of the normal brain parenchyma (1.02×10^{-3} mm^2/s). Abbreviation: ADC, apparent-diffusion-coefficient.

last two decades. Applications of DWI had been limited to CNS due to effects of respiration, cardiac movement, peristalsis and blood flow may effect on image quality in these parts of the body (11). Some technologic advances as echo-planar imaging, parallel imaging, and multichannel coils led to using of DWI in the extracranial sites such as abdomen and pelvis (3).

There is growing interest in the applications of DWI in oncologic area for last ten years. DWI has important advantages which require no contrast medium and long imaging time. Also it provides qualitative and quantitative information that can be helpful for tumor assessment. In this article, we present oncologic applications of DWI in the parts of the body.

Diffusion-weighted imaging in the CNS

Meningiomas are the most common extraaxial brain tumors. Meningiomas show characteristic findings on conventional MRI; thus, their differentiation from intraaxial tumors is easy. Hakyemez *et al.* (12) evaluated the contribution of DWI to differentiation of atypical/malignant and typical meningiomas. They demonstrated that atypical/malignant meningiomas had lower ADC values than typical meningiomas (*Figure 1*).

Conventional MRI cannot reliably distinguish epidermoid tumors from arachnoid cysts; since both lesions are very hyperintense relative to brain parenchyma on T2-weighted images and hypointense on T1-weighted images. With the combination of T2 and diffusion effect, epidermoid tumors are more hyperintense compared with cerebrospinal fluid (CSF) and brain tissue on DWI. Arachnoid cysts are fluid filled, demonstrate very high ADCs, and appear similar to CSF on DWI (13).

Gliomas are the most common primary neoplasms of the CNS. A number of studies showed that intraaxial tumors have higher ADC values than normal brain tissue (14-17) (*Figure 2*). Various investigators suggested that DWI be used in differentiation between high and low grade gliomas or between tumor types (15-17). In contrast to these results, Server *et al.* (18) suggested that differentiation between low

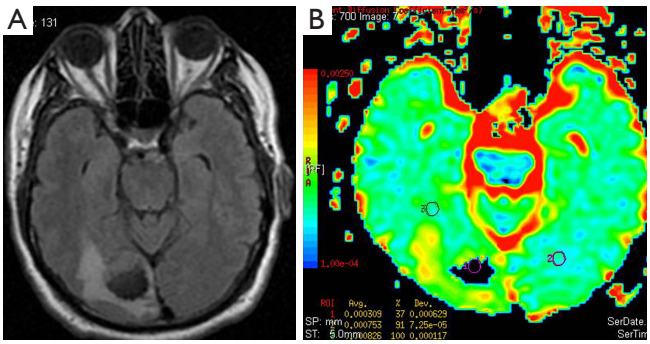

Figure 3 A 60-year old man with primary bladder cancer and brain metastasis. (A) FLAIR image shows right occipital metastasis and peritumoral vasogenic edema; (B) Color ADC map. ROI 1 shows the lesion and, ROI 2, 3 show normal parenchyma. ADC value of the metastasis was lower than ADC values of normal parenchyma. Abbreviations: ADC, apparent-diffusion-coefficient; ROI, region of interest.

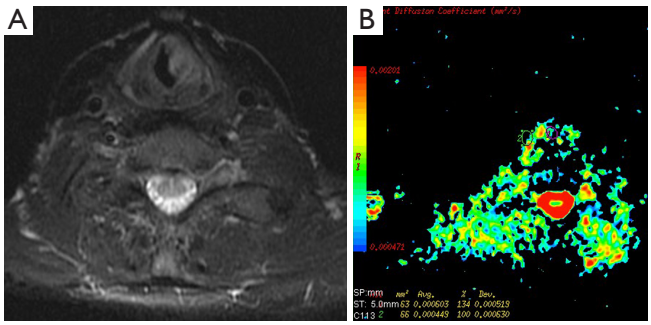

Figure 4 Primary left subglottic cancer. (A) Fat saturated axial T2 weighted image shows hyperintense mass protruded to the airway lumen; (B) Color ADC map. ROI 1 shows the tumor. The mass has higher ADC value than ADC value of normal laryngeal tissue. Abbreviations: ADC, apparent-diffusion-coefficient; ROI, region of interest.

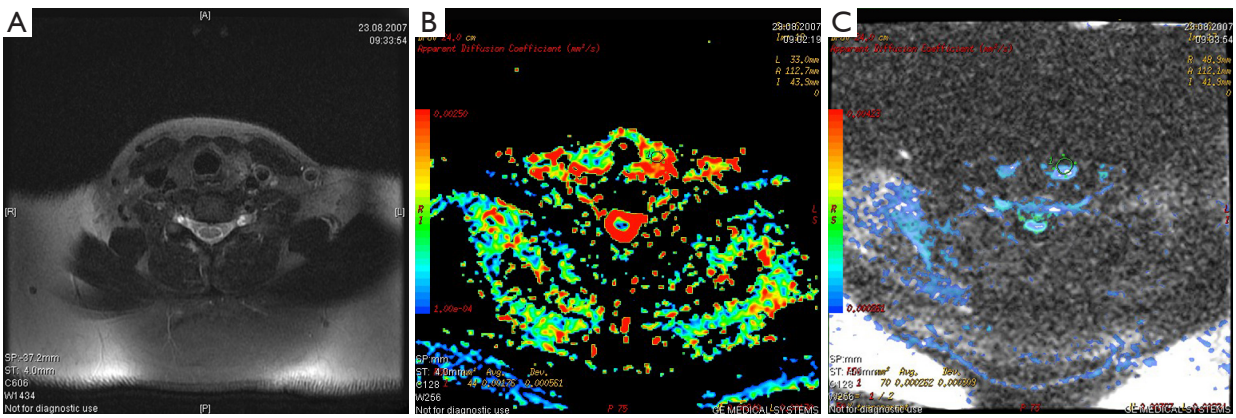

Figure 5 (A) Axial T2 images of malignant nodule. The nodule has increased signal intensity than normal tissue of thyroid; (B,C) Axial color ADC maps (by using a *b* value of 300) of benign (B) and malignant nodule (C) in the same level of axial T2 images, respectively. Malignant nodule has lower ADC values than benign nodule. ADC values of malignant and benign nodules are 0.2×10^{-3} and 1.76×10^{-3} mm^2/s, respectively. Abbreviation: ADC, apparent-diffusion-coefficient.

and high grade gliomas is possible using ADC measurement.

Metastasis is the most common intracranial tumor in adults. The most common metastasize to the brain are lung, breast, skin, genitourinary tract (*Figure 3*), colon and rectum, and paranasal sinus (19). Kono *et al.* (20) studied 21 patients with metastasis and have found a mean ADC value of 0.78×10^{-3} mm^2/s (used *b* 1,000 s/mm^2 gradient). ADC values of the metastasis were not statistically significant from glioblastomas. Duygulu *et al.* (21) evaluated the 76 patients with intracerebral metastasis using DWI. ADC value in metastasis showing restricted diffusion was 0.72×10^{-3} mm^2/s (used *b* 1,000 s/mm^2 gradient).

DWI has also important role in the evaluation of extracranial tumors such as thyroid (22), orbit and head and neck tumors (*Figure 4*). We studied the diagnostic role of DWI in differentiating of malignant and benign thyroid nodules. Mean ADC values of malignant and benign nodules were 0.96×10^{-3} mm^2/s and 3.06×10^{-3} mm^2/s for *b*-100, respectively. Mean ADC values of malignant nodules were lower than benign nodules for all *b* values. We concluded that DWI may be helpful in differentiating malignant and benign thyroid nodules (22) (*Figure 5*).

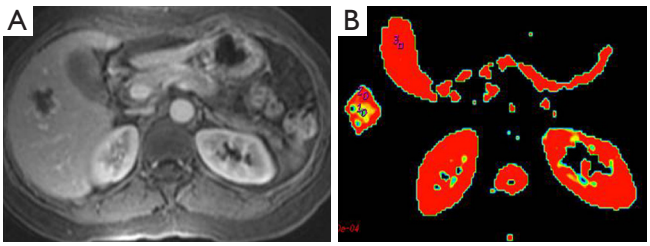

Figure 6 Right lobe liver hemangioma proven by imaging findings. (A) Axial contrast-enhanced T1 weighted image shows peripheral enhancement lesion in phase of the late arterial; (B) Color ADC map show placement of the ROIs in the lesion and normal parenchyma. ADC values of hemangioma and normal parenchyma (using *b* 600) are 1.26×10^{-3} and 1.83×10^{-3} mm^2/s. Abbreviations: ADC, apparent-diffusion-coefficient; ROI, region of interest.

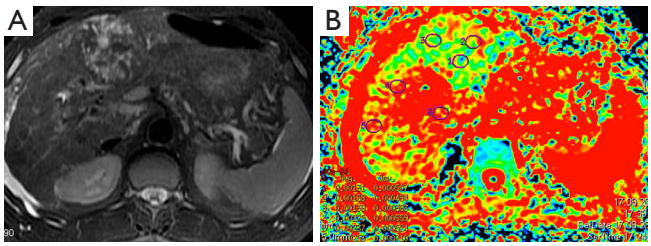

Figure 7 A 52-year old man with hepatoma proven by histopathologically. (A) Axial T2 weighted image shows heterogenous hyperintense lesion in the right liver lobe; (B) Axial color ADC map (by using b 600). ROI 1-3 located in the lesion and ROI 4-6 located in the normal parenchyma. ROI 1-3 show lower ADC values than normal parenchyma (ROI 4-6). Abbreviations: ADC, apparent-diffusion-coefficient; ROI, region of interest.

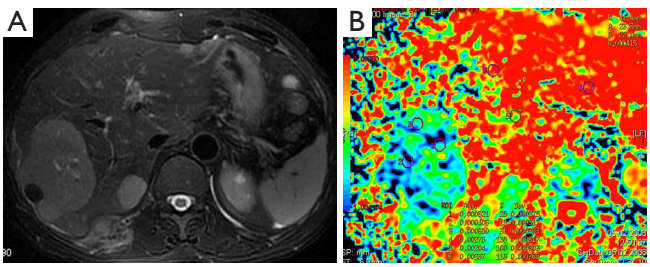

Figure 8 A 62-year old man with liver metastases from renal cell carcinoma. (A) Axial T2 weighted image show hyperintense two metastatic focus in the posterior liver lobe; (B) Color ADC map. ROI 1-3 located in the metastasis. Other ROIs show ADC values of the normal liver parenchyma. Metastasis has lower ADC values than normal liver tissue. Abbreviations: ADC, apparent-diffusion-coefficient; ROI, region of interest.

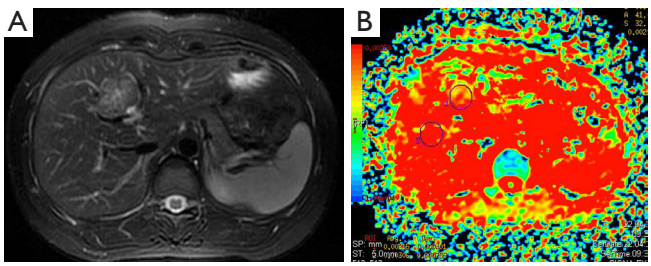

Figure 9 A 26-year old woman with focal nodular hyperplasia histopathological diagnosed. (A) Fat-supressed T2-weighted image shows hyperintense lesion in the right anterior liver lobe; (B) Color ADC map. In spite of the FNH is accepted as a benign lesion, lower ADC value is shown in the lesion. Abbreviations: ADC, apparent-diffusion-coefficient; FNH, focal nodular hyperplasia.

Diffusion-weighted imaging in the body

Liver pathologies were studied using DWI in many literatures (23-25). They concluded that ADC measurements can be used in the differential diagnosis of liver pathologies.

Liver hemangioma is the most common benign tumors of the liver. Hemangiomas are characterized by an enlargement of the extracellular space compared to normal tissue. So, hemangiomas have increased ADC values (26) (*Figure 6*). Moteki *et al.* (25) reported that mean ADC value of hemangioma (used following *b* values 3, 50 and 300) was 2.23×10^{-3} mm^2/s. Demir *et al.* (27) mentioned that mean ADC value of hemangioma (used *b* 1,000 s/mm^2 gradient) was 2.46×10^{-3} mm^2/s. According to our study mean ADC value of 61 hemangiomas was 1.98×10^{-3} mm^2/s for *b*-600 (28).

Hepatoma (*Figure 7*), metastasis (*Figure 8*) and focal nodular hyperplasia (FNH) (*Figure 9*) have lower ADC values than normal parenchyma. In recent study, Miller *et al.* (29) evaluated the ADC values for characterization of a variety of focal liver lesions. Mean ADC values (used *b*-0 and *b*-500 s/mm^2 gradients) of hepatoma, metastasis and FNH were 1.53×10^{-3} mm^2/s, 1.50×10^{-3} and 1.79×10^{-3} mm^2/s, respectively. They concluded that benign lesions have higher ADC values than malignant lesions. However, ADC value of benign lesion (FNH) is similar to malignant lesion.

Demir *et al.* (27) evaluated the diagnostic role of DWI in differentiation between benign and malignant liver lesions. Mean ADC values (used *b*-0 and *b*-500 s/mm^2 gradients) of hepatoma and metastases were 0.90×10^{-3}, and 0.79×10^{-3} mm^2/s, respectively. They concluded that DWI

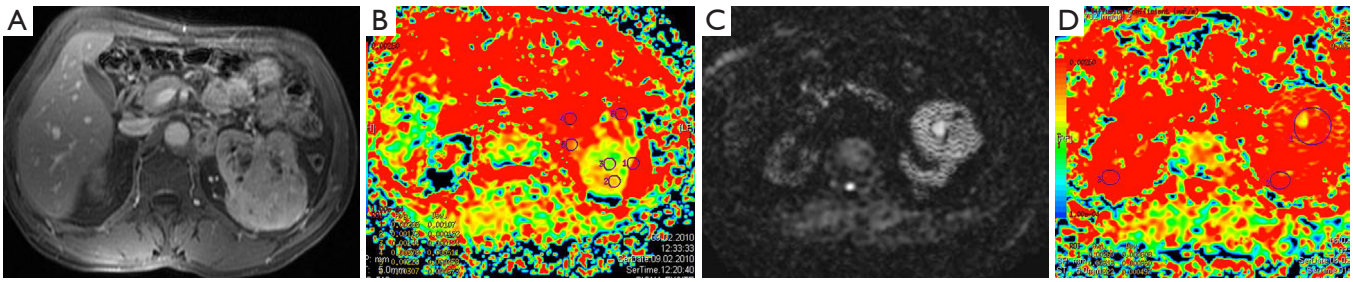

Figure 10 A 63-year old man with left RCC. (A) Contrast enhanced axial T1weighted image shows prominent enhancement of the lesion except cystic areas; (B) Color ADC map and ADC values. ROIs 2, 3 were located solid component of the lesion. ROI 1 shows cystic area and ROI 4-6 show normal renal parenchyma. ADC values of solid component lower than cystic and normal renal parenchyma. ADC values of tumor tissue are 1.44×10^{-3} and 1.73×10^{-3} mm^2/s; (C,D) A 73-year old women with renal oncocytoma; (C) DWI (used *b* 600 gradient value) shows restricted diffusion in the lesion; (D) Color ADC map. ADC value of oncocytoma is 2.60×10^{-3} mm^2/s. RCC has lower ADC values than oncocytoma. Abbreviations: RCC, renal cell carcinoma; ADC, apparent-diffusion-coefficient; ROI, region of interest; DWI, diffusion-weighted-imaging.

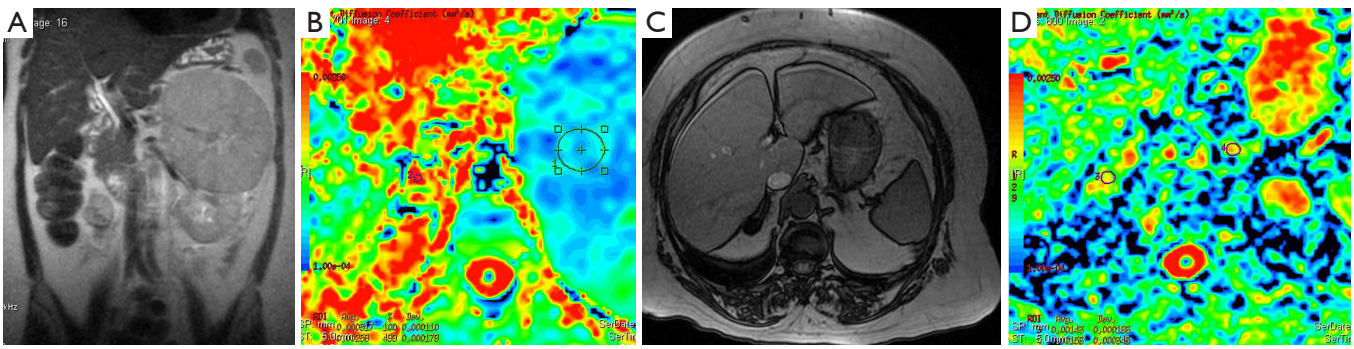

Figure 11 Huge left surrenal carcinoma proven histopathologically. (A) Coronal T2 weighted image shows isointense mass compared to renal parenchyma. Left kidney is compressed by the mass; (B) Color ADC map. ROI 1 shows ADC value of surrenal carcinoma has very low ADC values than normal surrenal parenchyma; (C,D) Right surrenal adenoma; (C) Axial out of the phase image shows prominent signal loss of the lesion consistent with adenoma; (D) Color ADC map reveals higher ADC values of adenoma than the adrenal carcinoma. Abbreviations: ADC, apparent-diffusion-coefficient; ROI, region of interest.

can be useful in the differentiation of benign and malignant liver lesions.

There are many studies related to diagnostic utility of DWI in the renal tumors. Malignant tumors have lower ADC values than benign ones (*Figure 10*). Restricted diffusion in renal neoplasms is probably multifactorial. It is related to cell membrane integrity and tissue cellularity (30). Taouli *et al.* (31) characterized renal lesions using DWI. The mean ADC value (used *b*-0, *b*-400 and *b*-800 s/mm^2 gradients) of 28 renal cell carcinomas (RCC) (1.41×10^{-3} mm^2/s) was significantly lower than benign lesions (2.23×10^{-3} mm^2/s). Cutoff ADC value for the diagnosis of RCC was less than or equal to 1.92×10^{-3} mm^2/s. They also mentioned that renal oncocytomas had significantly higher ADCs compared with solid RCC. Mean ADC value of oncocytomas reported as 1.91×10^{-3} mm^2/s. They concluded that DWI can be used to characterize renal lesions especially; it can be used to differentiate solid RCC from oncocytomas.

Adrenal masses are commonly detected on computed tomography (CT). Chemical shift MRI is useful in differentiating adenoma from nonadenoma. There is limited study related to usefulness of DWI in malignant tumors. Usually malignant tumors show bright signal on DWIs, and ADC values of malignant tumors are lower than benign tumors (*Figure 11*). Tsushima *et al.* (32) evaluated the diagnostic utility of DWI for the diagnosis of adrenal tumors. They found no difference in ADC values between adenomas and metastatic tumors. However, pheochromocytomas had higher mean ADC value

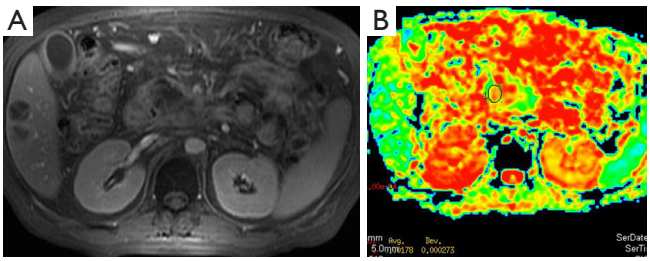

Figure 12 A 48-year old man with inoperable pancreas carcinoma liver metastases. (A) Contrast enhanced fat saturated T1 weighted axial image shows heterogen enhanced huge mass in head and corpus of the pancreas; (B) ADC value of the mass is 1.78×10^{-3} mm^2/s. ADC value of the normal appearing parenchyma is 2.97×10^{-3} mm^2/s (not shown). Abbreviation: ADC, apparent-diffusion-coefficient.

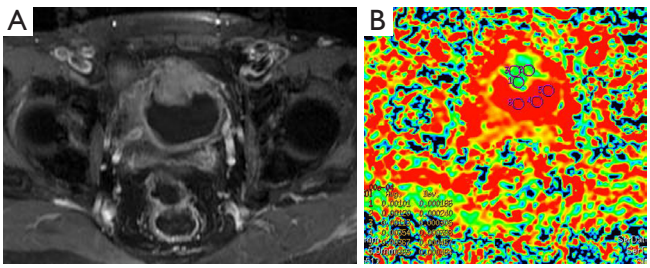

Figure 14 A 67-year old man with bladder cancer diagnosed six month ago. (A) Contrast enhanced T1 axial image shows polypoid mass located anterior bladder wall; (B) Color ADC map. Similar to other related studies, bladder cancer has lower ADC values than normal wall. Mean ADC value of this case is 1.11×10^{-3} mm^2/s in the cancerous tissue. Abbreviation: ADC, apparent-diffusion-coefficient.

compared with those of adenomas and metastasis.

Diagnosis of pancreatic cancer is delayed in many cases and very few patients have curative surgical treatment. Pancreatic cancer has an unfavourable overall 5-year survival of about 5% (33). Similar to other malignant tumors, it has lower ADC value compared to normal pancreatic tissue (*Figure 12*). ADC values of pancreatic cancer were in wide range with overlapping normal pancreatic tissue values. This may be due to histopathological components of pancreatic cancer which contain varying degrees of fibrosis, necrosis, mucin and cellular component (34). Recent studies concluded that restricted diffusion in the pancreatic cancer might be related with increased cellularity and fibrosis. In contrast to other tumors, fibrosis might be contributed to diminished ADC values as well as cellularity (34).

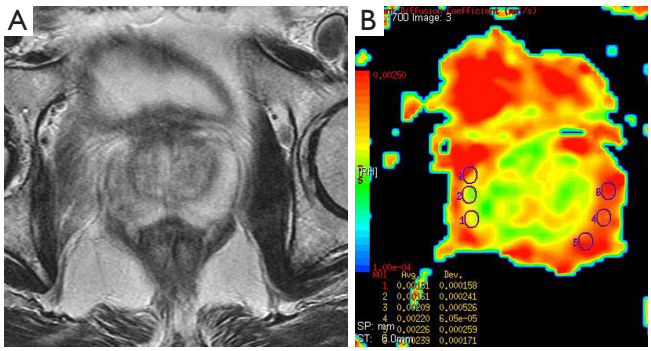

Figure 13 A 62-year old man with prostate carcinoma diagnosed by histopathologically. (A) Axial T2 weighted image shows hypointense area in right peripheral zone compared to left peripheral zone; (B) Color ADC map. Settlement of the ROIs in area of right and left peripheral zones. ADC values of the malignant areas lower than left peripheral zone of the prostate. Abbreviations: ADC, apparent-diffusion-coefficient; ROI, region of interest.

Prostate cancer is the most common genitourinary malignancy in men (35). There were many literature related to diagnostic utility of DWI in prostate cancer (35-38). Prostate cancer usually demonstrates low signal intensity on T2-weighted image that is well identified in the peripheral zone from the normal appearance of high signal intensity on T2-weighted image. In prostate cancer, normal tissue of the gland is replaced by adenocarcinoma. The tumor is built up of high-density malignant epithelial cells, which results a decrease in ADC values (36) (*Figure 13*). Kiliçkesmez *et al.* (35) measured the mean ADC value (used *b*-0, *b*-500 and *b*-1,000 s/mm^2 gradients) of prostate tissue in nine prostate cancer and 50 healthy subjects. Mean ADC value of peripheral and transitional zone of prostate were 2.07×10^{-3} and 1.46×10^{-3} mm^2/s, respectively. Mean ADC value of prostate carcinoma was 1.06×10^{-3} mm^2/s. Yağci *et al.* (37) investigated the value of DWI for prostate cancer detection and localization. They found lower ADC value in prostate cancer than noncancerous tissue. Mean ADC values (used *b*-800 s/mm^2 gradient) of cancerous and noncancerous tissues were 0.94×10^{-3} and 1.58×10^{-3} mm^2/s, respectively.

Carcinoma of the urinary bladder is one of the most common malignant tumors of the urinary tract. In the literature, there are a few reports evaluating the feasibility of DWI in the diagnosis of urinary bladder cancers (*Figure 14*). Matsuki *et al.* (39) reported that the ADC value of bladder cancers was lower than ADC value of normal bladder wall. They suggested that the bladder cancers were clearly

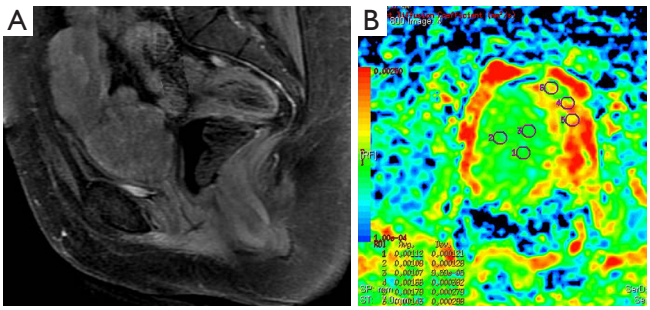

Figure 15 A 43-year old woman with high grade cervix cancer. (A) Contrast enhanced sagittal T1 weighted image shows heterogenous enhanced huge cervical mass; (B) Color ADC map. ADC values of ROIs 1-3 located in the tumoral tissue were lower than ADC values of normal tissue. Abbreviations: ADC, apparent-diffusion-coefficient; ROI, region of interest.

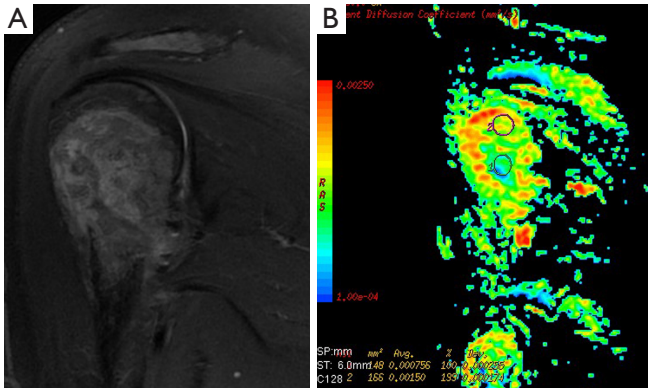

Figure 16 A 32-year old man with giant cell tumor of the humerus. (A) The lesion is hyperintense at T2 weighted coronal image; (B) Color ADC map. ROI 1 shows in the lesion and ROI 2 shows normal area. An ADC value of tumor is higher than normal parenchyma. Abbreviations: ADC, apparent-diffusion-coefficient; ROI, region of interest.

detected using DWI. However, they did not define a cut-off value. El-Assmy *et al.* (40) reported high sensitivity and specificity of DWI in detection of bladder tumors depending on their site. In another study, the mean ADC values (used *b*-0, *b*-500 and *b*-1,000 s/mm^2 gradients) of the urinary bladder wall of the control group and bladder carcinoma were 2.08×10^{-3} and 0.94×10^{-3} mm^2/s, respectively. They concluded that ADC measurement has a potential ability to differentiate carcinomas from normal bladder wall (35).

DWI is also widely used in evaluation of pelvic region tumors. Similar to other malignant tumors, the ADC values of uterine cancers are lower than normal tissue (*Figure 15*). ADC value provides useful information about the effectiveness of the therapy as well as differentiation of between malignant tumor tissue and normal tissue. Naganawa *et al.* (41) reported that mean ADC value (used *b*-0, *b*-300 and *b*-600 s/mm^2 gradients) of cervical cancer was lower than of normal cervical tissue (1.09×10^{-3} *vs.* 1.79×10^{-3} mm^2/s). In another study carried by McVeigh *et al.* (42) with larger group of cervical cancer, mean ADC values (used *b*-0, *b*-600 s/mm^2 gradients) of cervical cancer and normal tissue were reported 1.09×10^{-3} *vs.* 2.09×10^{-3} mm^2/s, respectively. These studies suggested that ADC measurement has a potential ability to differentiate between cancerous and normal tissue. There are many reports about the role of DWI in the diagnosis of cystic ovarian tumors. The cystic components of malignant ovarian cystic tumors had lower ADC values than other benign ovarian cysts, except hemorrhagic cysts and cystic neoplasms (43). However, Nakayama *et al.* (44) found no significant difference between ADC values of benign and malignant cystic neoplasms. They concluded that it is difficult to identify the ADC threshold value for differentiation among cystic ovarian tumors.

Diffusion-weighted imaging in the bone and lung tumors

There are limited reports about diagnostic utility of DWI related to bone tumors. Many reports focused on vertebral body. Typical values of the ADC in normal bone marrow are in the range of 0.2×10^{-3}-0.5×10^{-3} mm^2/s. Most applications of DWI in the bone marrow are focused on the differentiation of benign osteoporotic and malignant vertebral compression fractures (45,46). According to our study mean ADC values of sacral and iliac bone marrow were 0.53×10^{-3} and 0.56×10^{-3} mm^2/s at *b*-1,000 (47). ADC values (used *b*-500 s/mm^2 gradient) of pathologic bone marrow range between 0.7×10^{-3} to 1.0×10^{-3} mm^2/s in metastases and malignant vertebral fractures (48). Although ADC values may be indicative for benign (*Figure 16*) or malignant lesions, a considerable overlap between mean ADC values of benign and malignant lesions has been described in several studies (49).

A solitary pulmonary nodule is a common condition in clinical practice. CT and PET (positron emission tomography) are common used modalities as noninvasive imaging methods. Some investigators have tried to discriminate malignancy from benign lung tumors by measuring ADC value. Mori *et al.* (50) examined

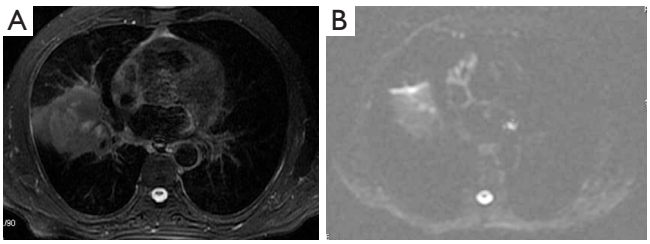

Figure 17 A 71-year old man with malignant lung cancer. (A) Fat saturated T2 weighted axial image shows hyperintense irregular lesion located on middle lung lobe; (B) DWI shows restricted diffusion of the lesion. Abbreviation: DWI, diffusion-weighted-imaging.

the usefulness of DWI for discrimination of benign/malignant pulmonary nodules in comparison with F-fluorodeoxyglucose (PET). The receiver operating characteristics curve showed cutoff values of the ADC for benign/malignant discrimination to be 1.1×10^{-3} mm^2/s. Similarity to other systems, malignant pulmonary nodules has low ADC values (*Figure 17*).

In conclusion

DWI is a useful technique that provides information about cellularity and cell membrane architecture of tumoral tissue. One of the most prominent contributions of DWI is differentiation between malignant and benign tumoral process. Despite many reports which present cut off values for differentiation between benign and malignant processes, many authors mentioned that overlapping ADC values exist in benign and malignant tumors. However, most of the studies suggested that malignant tumors had lower ADC values than benign ones. DWI is also useful to assess the response of tumors to treatment in various parts of the body. Combination of conventional MRI, DWI and ADC values provides additional information in patients with cancers. The most prominent advantages of this technique are absence of radiation, no necessity for of intravenous contrast material, very quick technique and quantitative information of tissue provided by ADC measurement. DWI may be a routine sequence in oncologic settings and it provides much useful information about tumoral tissue. We think it can be added to conventional MRI sequences.

Acknowledgements

Disclosure: The authors declare no conflict of interest.

References

1. Bammer R. Basic principles of diffusion-weighted imaging. Eur J Radiol 2003;45:169-84.
2. Le Bihan D, Breton E, Lallemand D, et al. Separation of diffusion and perfusion in intravoxel incoherent motion MR imaging. Radiology 1988;168:497-505.
3. Koh DM, Collins DJ. Diffusion-weighted MRI in the body: applications and challenges in oncology. AJR Am J Roentgenol 2007;188:1622-35.
4. Thoeny HC, De Keyzer F, Vandecaveye V, et al. Effect of vascular targeting agent in rat tumor model: dynamic contrast-enhanced versus diffusion-weighted MR imaging. Radiology 2005;237:492-9.
5. Gauvain KM, McKinstry RC, Mukherjee P, et al. Evaluating pediatric brain tumor cellularity with diffusion-tensor imaging. AJR Am J Roentgenol 2001;177:449-54.
6. Wang J, Takashima S, Takayama F, et al. Head and neck lesions: characterization with diffusion-weighted echo-planar MR imaging. Radiology 2001;220:621-30.
7. Anderson JR, Tumours I. General features, types and examples. In: Anderson JR, eds. Muir's textbook of pathology. 20th ed. London: Edward Arnold, 2001:12.1-12.49.
8. Thoeny HC, De Keyzer F, Chen F, et al. Diffusion-weighted MR imaging in monitoring the effect of a vascular targeting agent on rhabdomyosarcoma in rats. Radiology 2005;234:756-64.
9. Byun WM, Shin SO, Chang Y, et al. Diffusion-weighted MR imaging of metastatic disease of the spine: assessment of response to therapy. AJNR Am J Neuroradiol 2002;23:906-12.
10. Chen CY, Li CW, Kuo YT, et al. Early response of hepatocellular carcinoma to transcatheter arterial chemoembolization: choline levels and MR diffusion constants--initial experience. Radiology 2006;239:448-56.
11. Müller MF, Prasad P, Siewert B, et al. Abdominal diffusion mapping with use of a whole-body echo-planar system. Radiology 1994;190:475-8.
12. Hakyemez B, Yildirim N, Gokalp G, et al. The contribution of diffusion-weighted MR imaging to distinguishing typical from atypical meningiomas. Neuroradiology 2006;48:513-20.
13. Schaefer PW, Grant PE, Gonzalez RG. Diffusion-weighted MR imaging of the brain. Radiology 2000;217:331-45.
14. Tien RD, Felsberg GJ, Friedman H, et al. MR imaging of high-grade cerebral gliomas: value of diffusion-weighted echoplanar pulse sequences. AJR Am J Roentgenol

1994;162:671-7.
15. Brunberg JA, Chenevert TL, McKeever PE, et al. In vivo MR determination of water diffusion coefficients and diffusion anisotropy: correlation with structural alteration in gliomas of the cerebral hemispheres. AJNR Am J Neuroradiol 1995;16:361-71.
16. Eis M, Els T, Hoehn-Berlage M, et al. Quantitative diffusion MR imaging of cerebral tumor and edema. Acta Neurochir Suppl 1994;60:344-6.
17. Eis M, Els T, Hoehn-Berlage M. High resolution quantitative relaxation and diffusion MRI of three different experimental brain tumors in rat. Magn Reson Med 1995;34:835-44.
18. Server A, Kulle B, Gadmar OB, et al. Measurements of diagnostic examination performance using quantitative apparent diffusion coefficient and proton MR spectroscopic imaging in the preoperative evaluation of tumor grade in cerebral gliomas. Eur J Radiol 2011;80:462-70.
19. Akeson P, Larsson EM, Kristoffersen DT, et al. Brain metastases--comparison of gadodiamide injection-enhanced MR imaging at standard and high dose, contrast-enhanced CT and non-contrast-enhanced MR imaging. Acta Radiol 1995;36:300-6.
20. Kono K, Inoue Y, Nakayama K, et al. The role of diffusion-weighted imaging in patients with brain tumors. AJNR Am J Neuroradiol 2001;22:1081-8.
21. Duygulu G, Ovali GY, Calli C, et al. Intracerebral metastasis showing restricted diffusion: correlation with histopathologic findings. Eur J Radiol 2010;74:117-20.
22. Bozgeyik Z, Coskun S, Dagli AF, et al. Diffusion-weighted MR imaging of thyroid nodules. Neuroradiology 2009;51:193-8.
23. Ichikawa T, Haradome H, Hachiya J, et al. Diffusion-weighted MR imaging with a single-shot echoplanar sequence: detection and characterization of focal hepatic lesions. AJR Am J Roentgenol 1998;170:397-402.
24. Koh DM, Scurr E, Collins DJ, et al. Colorectal hepatic metastases: quantitative measurements using single-shot echo-planar diffusion-weighted MR imaging. Eur Radiol 2006;16:1898-905.
25. Moteki T, Horikoshi H. Evaluation of hepatic lesions and hepatic parenchyma using diffusion-weighted echo-planar MR with three values of gradient b-factor. J Magn Reson Imaging 2006;24:637-45.
26. Gourtsoyianni S, Papanikolaou N, Yarmenitis S, et al. Respiratory gated diffusion-weighted imaging of the liver: value of apparent diffusion coefficient measurements in the differentiation between most commonly encountered benign and malignant focal liver lesions. Eur Radiol 2008;18:486-92.
27. Demir OI, Obuz F, Sagol O, et al. Contribution of diffusion-weighted MRI to the differential diagnosis of hepatic masses. Diagn Interv Radiol 2007;13:81-6.
28. Bozgeyik Z, Kocakoc E, Gul Y, et al. Evaluation of liver hemangiomas using three different b values on diffusion MR. Eur J Radiol 2010;75:360-3.
29. Miller FH, Hammond N, Siddiqi AJ, et al. Utility of diffusion-weighted MRI in distinguishing benign and malignant hepatic lesions. J Magn Reson Imaging 2010;32:138-47.
30. Hayashida Y, Hirai T, Morishita S, et al. Diffusion-weighted imaging of metastatic brain tumors: comparison with histologic type and tumor cellularity. AJNR Am J Neuroradiol 2006;27:1419-25.
31. Taouli B, Thakur RK, Mannelli L, et al. Renal lesions: characterization with diffusion-weighted imaging versus contrast-enhanced MR imaging. Radiology 2009;251:398-407.
32. Tsushima Y, Takahashi-Taketomi A, Endo K. Diagnostic utility of diffusion-weighted MR imaging and apparent diffusion coefficient value for the diagnosis of adrenal tumors. J Magn Reson Imaging 2009;29:112-7.
33. Jemal A, Siegel R, Ward E, et al. Cancer statistics, 2008. CA Cancer J Clin 2008;58:71-96.
34. Muraoka N, Uematsu H, Kimura H, et al. Apparent diffusion coefficient in pancreatic cancer: characterization and histopathological correlations. J Magn Reson Imaging 2008;27:1302-8.
35. Kiliçkesmez O, Cimilli T, Inci E, et al. Diffusion-weighted MRI of urinary bladder and prostate cancers. Diagn Interv Radiol 2009;15:104-10.
36. Chen M, Dang HD, Wang JY, et al. Prostate cancer detection: comparison of T2-weighted imaging, diffusion-weighted imaging, proton magnetic resonance spectroscopic imaging, and the three techniques combined. Acta Radiol 2008;49:602-10.
37. Yağci AB, Ozari N, Aybek Z, et al. The value of diffusion-weighted MRI for prostate cancer detection and localization. Diagn Interv Radiol 2011;17:130-4.
38. Iwazawa J, Mitani T, Sassa S, et al. Prostate cancer detection with MRI: is dynamic contrast-enhanced imaging necessary in addition to diffusion-weighted imaging? Diagn Interv Radiol 2011;17:243-8.
39. Matsuki M, Inada Y, Tatsugami F, et al. Diffusion-weighted MR imaging for urinary bladder carcinoma: initial results. Eur Radiol 2007;17:201-4.

40. El-Assmy A, Abou-El-Ghar ME, Refaie HF, et al. Diffusion-weighted MR imaging in diagnosis of superficial and invasive urinary bladder carcinoma: a preliminary prospective study. ScientificWorldJournal 2008;8:364-70.
41. Naganawa S, Sato C, Kumada H, et al. Apparent diffusion coefficient in cervical cancer of the uterus: comparison with the normal uterine cervix. Eur Radiol 2005;15:71-8.
42. McVeigh PZ, Syed AM, Milosevic M, et al. Diffusion-weighted MRI in cervical cancer. Eur Radiol 2008;18:1058-64.
43. Katayama M, Masui T, Kobayashi S, et al. Diffusion-weighted echo planar imaging of ovarian tumors: is it useful to measure apparent diffusion coefficients. J Comput Assist Tomogr 2002;26:250-6.
44. Nakayama T, Yoshimitsu K, Irie H, et al. Diffusion-weighted echo-planar MR imaging and ADC mapping in the differential diagnosis of ovarian cystic masses: usefulness of detecting keratinoid substances in mature cystic teratomas. J Magn Reson Imaging 2005;22:271-8.
45. Baur A, Stäbler A, Brüning R, et al. Diffusion-weighted MR imaging of bone marrow: differentiation of benign versus pathologic compression fractures. Radiology 1998;207:349-56.
46. Taskin G, Incesu L, Aslan K. The value of apparent diffusion coefficient measurements in the differential diagnosis of vertebral bone marrow lesions. Turk J Med Sci 2013;43:379-87.
47. Bozgeyik Z, Ozgocmen S, Kocakoc E. Role of diffusion-weighted MRI in the detection of early active sacroiliitis. AJR Am J Roentgenol 2008;191:980-6.
48. Dietrich O, Biffar A, Reiser MF, et al. Diffusion-weighted imaging of bone marrow. Semin Musculoskelet Radiol 2009;13:134-44.
49. Biffar A, Dietrich O, Sourbron S, et al. Diffusion and perfusion imaging of bone marrow. Eur J Radiol 2010;76:323-8.
50. Mori T, Nomori H, Ikeda K, et al. Diffusion-weighted magnetic resonance imaging for diagnosing malignant pulmonary nodules/masses: comparison with positron emission tomography. J Thorac Oncol 2008;3:358-64.

Cite this article as: Bozgeyik Z, Onur MR, Poyraz AK. The role of diffusion weighted magnetic resonance imaging in oncologic settings. Quant Imaging Med Surg 2013;3(5):269-278. doi: 10.3978/j.issn.2223-4292.2013.10.07

